A LOW COST, HIGH RESOLUTION ACOUSTIC CAMERA WITH A FLEXIBLE MICROPHONE CONFIGURATION

Rick van der Goot[1], Jorg Hendriks[1], Kirk Scheper[1], Giel Hermans[2], Wouter van der Wal[1] and Dick G. Simons[1]

[1]Faculty of Aerospace Engineering, Delft University of Technology
Kluyverweg 1, 2629 HS Delft, The Netherlands
[2]Department DEMO-CEO, Delft University of Technology
Mekelweg 4, 2628CD Delft, The Netherlands

ABSTRACT

The need for aircraft noise reduction is acknowledged worldwide. Acoustic cameras play an important role to identify aircraft noise sources. An acoustic camera tailored for aircraft noise was designed, built and tested by students of the Faculty of Aerospace Engineering of Delft University of Technology. The camera uses only 32 microphones, while still maintaining a high angular resolution. The design resulted in an acoustic camera tailored for measuring aircraft noise with a flexible array configuration and array aperture due to a clever mechanical construction. The system is easily transportable and has a short set up time (less than half an hour). The specifications of the acoustic camera are comparable to existing commercial ones. Various beamforming methods were implemented: conventional least-squares-based beamforming, Capon beamforming, the MUSIC algorithm and so-called CLEAN-PSF and CLEAN-SC. Due to its versatility, the camera can also be used for other applications, such as abatement of traffic and industrial noise and architectural and room acoustics. The developed acoustic camera was tested by measuring fly-over noise of landing aircraft. Despite its low cost design, the camera proved to have the required angular resolution to clearly distinguish between engine and airframe noise.

1   INTRODUCTION

Noise pollution has been a problem for residents living close to airports for many years. In the last few decades aircraft engines were the main emitters of noise, but over the years these became considerably quieter, to such an extent that the noise generated by the airflow over the airplane, i.e. airframe noise, can have roughly the same sound pressure level as engine noise. To further reduce the noise emission of aircraft noise in the next decade, all noise sources on an airplane need to be identified. A tool to localise individual aircraft noise sources is an acoustic camera. A drawback of current acoustic cameras is that they are usually expensive and not very flexible, which makes them limited in use.

In this paper the design, building and testing of a high resolution, low cost acoustic camera tailored to aircraft noise is presented. The camera, developed in a student project of the Faculty of Aerospace Engineering of Delft University of Technology, was designed to meet the following requirements:

- The camera consists of 32 microphones and various array configurations should be possible.
- The camera has an angular resolution of better than 1.5^{o} at 6000 Hz. This is based on the requirement that the camera should be able to distinguish between engine and airframe noise when an aircraft flies at 40 m altitude.
- The total cost of the camera should be below 7500 Euro.
- The camera has an online display facility.
- The camera is able to operate up to a wind speed of 3 Beaufort.
- The camera can be transported in a minivan.
- The set up time is less than one hour when two people are handling the camera.

First, a detailed explanation of the different subsystems (mechanical structure, data acquisition system and data processing system) of the camera is described, followed by a discussion of tests performed with synthetic data. Next, tests on real aircraft flyovers are presented and discussed. The final specifications of the camera are listed in the conclusions.

2   MECHANICAL STRUCTURE

The mechanical design supports 32 microphones in a reconfigurable array with a size of 2.32 by 1.56 m. The structure is constructed using commercial off-the-shelf components. The general concept consists of three parts: the supporting structure, the structure to which the microphones will be attached (here called the array structure) and the microphone connection to the array structure. A description of the first two parts will be given below.

The frame of a pop-up stand is used as supporting structure. This frame is shown in figure 2.1. It consists of aluminium tubes which can rotate with respect to each other. The structure can be folded or unfolded using these rotations. This frame was chosen for its very fast set-up and its small volume during transport.

Figure 2.1   Supporting structure of the acoustic camera.

A structure to carry the microphones is attached to this frame. For this, use was made of six wooden plates (see figure 2.1), which can be attached to and detached from the frame. In these plates, 1350 holes are drilled for inserting the microphones. The shape of the array is flexible because of the large number of holes. The spacing between the holes is 5.2 cm, hence the maximum frequency that can be measured without aliasing is around 3.3 kHz. A small part of the holes has a spacing of 2.5 cm, which can be used for measurements at higher frequencies. Also some extra holes were added for a spiral-shaped array.

The resulting design is very flexible, which is why this camera can be used for several other applications besides aircraft noise measurements, e.g. for very high frequencies, a small array with a small microphone spacing can be used.

A disadvantage of this structure is sound reflection off the wooden plates, which can influence the measurements. Absorbing foam is attached to the plates to reduce this effect. Flamex Basic [1] foam was selected. The absorption coefficient of this foam is given in figure 2.2.
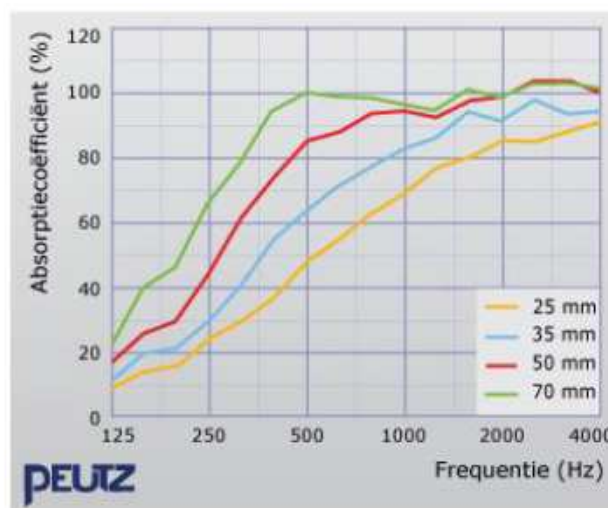
Figure 2.2   Absorption coefficient versus frequency of the Flamex Basic foam used to reduce sound reflections of the wooden plates.

3   DATA ACQUISITION SYSTEM

The dynamic range of the microphones is set to 60 - 126 dB. The received signal is fed into a PCB board, which subsequently consists of a high pass filter, an amplifier and a low pass filter. Also, jumpers are installed to be able to bypass a filter. The maximum output voltage of the microphones is 1 V, which corresponds to 129 dB, corresponding to the maximum level of 126 dB with a margin. The maximum input of the analogue to digital converters is 10 V, so the amplifier has a gain of 10. The low pass filter is used to cut off frequencies above 11 kHz [3], which is the maximum frequency of interest for airplanes. This is well below the Nyquist frequency at the sampling rate of 90 kHz.

Next, the signals are fed into the digital signal processor (DSP), which consists of a field-programmable gate array (FPGA) a real time (RT) controller and the host PC. This system carries out a set of predetermined tasks needed to digitize the signals from all microphones and transfer this data to the host PC. First, the FPGA transmits the data from the ADC cards as signed 16 bit integer values. (The calibration data, the LSB weight and the offset, is also transmitted to convert these raw data for use at a later stage). Then, the data is transferred to the RT controller, which transfers the recorded data from the FPGA to the host computer. The RT-controller is also used to send commands from the computer to the data acquisition system. Finally, the data enters the host PC, where the data is stored to be used by the beamforming algorithms. It is also possible to show the data (in the form of a calibrated power spectral analysis) in the LabVIEW software, e.g. for the purpose of ensuring that the measurement is valid.

An important parameter of the DSP is the sampling rate, which should at least be twice as high as the maximum frequency of interest, being 11 kHz. It was already stated that the sampling rate was chosen to be 90 kHz (having a safety margin with respect to the maximally possible sampling frequency of 100 kHz).

Sampling blocks of 20 ms are send to the host computer. Since the measured airplanes are moving, this short sample time can avoid blurring of the final image and effects due to changes in Doppler shift [4]. However, the frequency resolution is limited in that case. The 20 ms data blocks are processed separately in the beamforming algorithm.

4   DATA PROCESSING SYSTEM

Five beamforming methods were implemented, i.e., conventional beamforming [5], Capon beamforming [6], a MUSIC algorithm [7] and CLEAN-PSF [8] and CLEAN-SC [8]. As the results shown in this paper were all obtained with the conventional beamformer, only this beamformer is described briefly in the following.

Conventional beamforming is a narrowband algorithm performed in the frequency domain. Since it is a narrowband algorithm only one frequency can be processed at a time. The microphone amplitude and phase, called steering vector, are determined assuming a sound source of unit strength emitting the frequency of interest at a certain position. The actual sound intensity from that position can then be derived. This is repeated for a certain adjustable 3D scan region, subdivided in a point grid. This steering vector is given by

$$\bar{g}_s = \frac{-e^{-2\pi i f \Delta t(\bar{x}_m, \bar{x}_s)}}{4\pi \|\bar{x}_m - \bar{x}_s\|}$$

Eq. 4.1

where $\bar{x}_m$ is the microphone position vector, $\bar{x}_s$ is the assumed source position vector, Δt is the travel time of the signal between the source and the microphone and f is the frequency of interest. The denominator accounts for the amplitude decay. The microphone signals corresponding to the assumed source, $\bar{g}_s$, are compared to the actual microphone signals, $\bar{p}_m$, by minimizing $\|\bar{g}_s \cdot a_s - \bar{p}_m\|^2$. This is a least-squares problem the solution of which is given by

$$a_s = \frac{\vec{g}_s \cdot \bar{p}_m}{|\bar{g}_s|^2}$$

Eq. 4.2

being a complex number corresponding to the emitted signal at a certain point in the grid with relative amplitude $|a_s|$. The source power is determined using

$$P = \frac{1}{2}|a_s|^2$$

Eq. 4.3

The results for each grid point are stored in a matrix, which can be plotted as a source plot result. The amplitude decay factor amplifies the found scan point source powers according to their distance to the microphones. The outer scan points are therefore amplified more than the scan points in the centre of the plot. If a wide field of view is required it is sometimes preferable to leave out the amplitude decay factor, since it can amplify noise and aliasing effects at the outer scan points to levels above the actual source power levels in the centre of the plot. Moreover, the amplitude decay factor also shifts source maxima outward since the algorithm-induced width of a source is amplified more with increasing distance from the centre. However, it should be noted that without this factor the noise levels in the source plot lose their physical meaning, therefore the factor is kept in our processing.

5   ARRAY CONFIGURATION TESTS

Tests were performed to find an optimal configuration to measure aircraft noise. In these tests, aircraft noise was simulated and processed by the conventional beamformer [5] using five different array configurations. In this way, an attempt is made to find the optimal array configuration for the specific case of aircraft sound source identification.

These tests were done by simulating the engine sound and aerodynamic sound simultaneously. It is assumed that a turbojet engine emits sound in the band 1200-6000 Hz [2] and that aerodynamic sound can be found around 1000 Hz. Furthermore, the aircraft flyover measurements are made for aircraft altitudes of 40 m (section 6). Therefore, in the test one source was placed at position (-10 m, -10 m, 40 m), emitting sound at 1200 and 6000 Hz, whereas the other source was positioned at location (10 m, 15 m, 40 m) emitting sound at 1000 Hz. The signal was subsequently processed using the conventional beamformer. The results are displayed by means of a so-called source plot.

The following array configurations are analysed:

- Circular configuration
- Logarithmic configuration
- Rectangular configuration
- Spiral configuration

Each of these configurations was assessed based on the following criteria. The first criterion is resolution, measured using the maximum half power width of a source. The second criterion concerns the side lobes. The number of side lobes in the source plots that are above half the maximum power are counted. The final criterion is the precision. Because the exact sound source locations are known from the simulation, these can be compared with the sources obtained in the source plot. Calculating the average distance between the actual and the found location of both sources gives a clear indication of the precision.

The results are given in figures 5.1 to 5.4 below. For each of the array configurations given on the left in each figure the array aperture is virtually the same, i.e., 2 by 2 m.
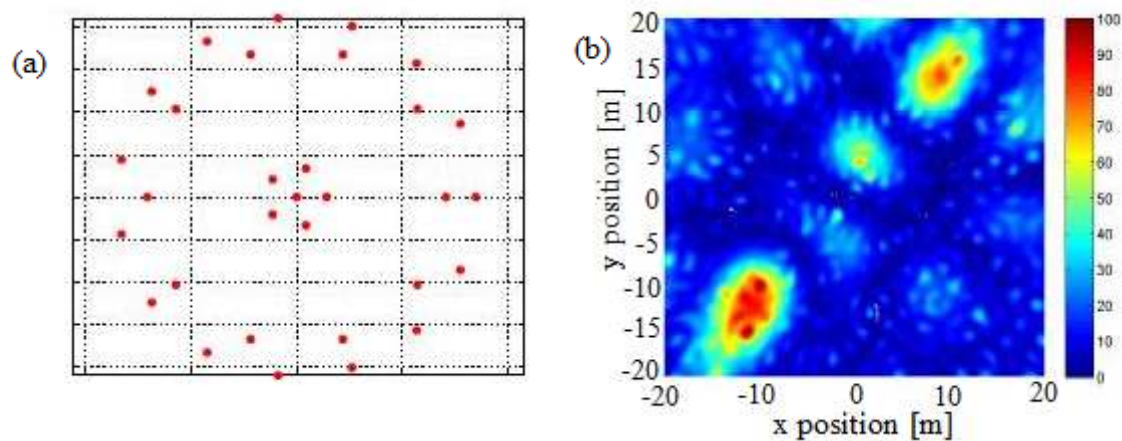
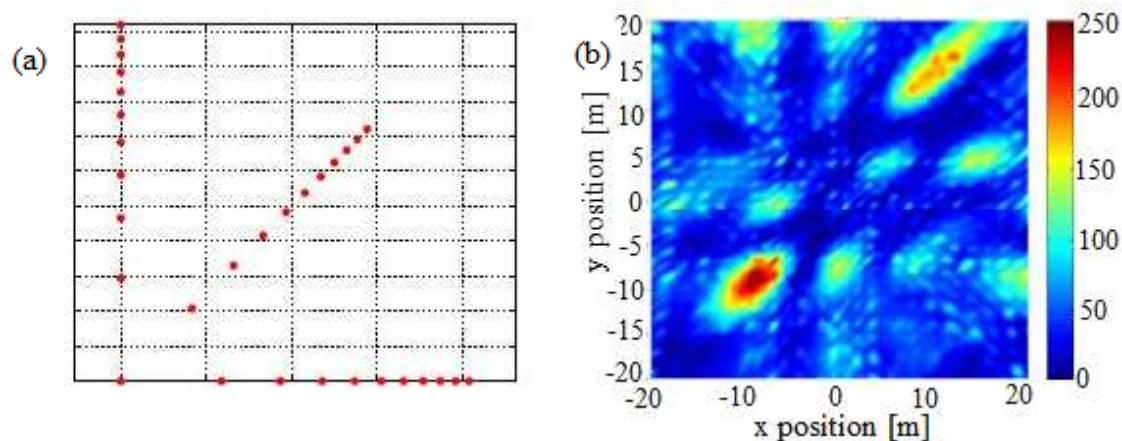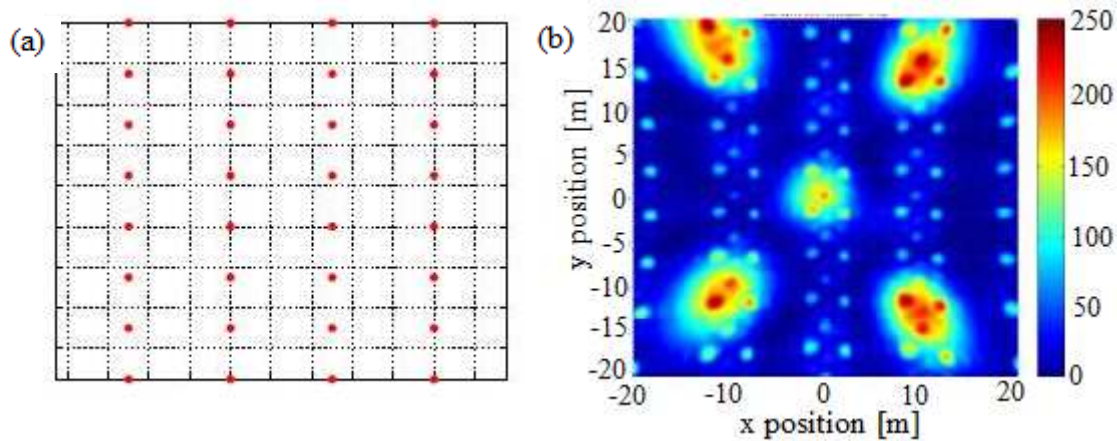*Figure 5.1*   *(a) Microphone configuration and (b) source plot for a circular array.*
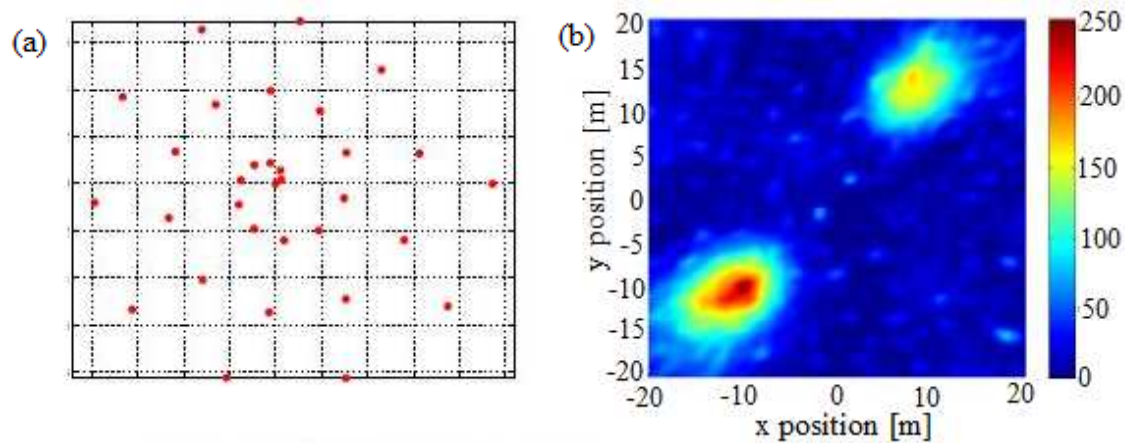

Figure 5.2   *(a) Microphone configuration and (b) source plot for a logarithmic array.*

Figure 5.3   (a) Microphone configuration and (b) source plot for a rectangular array.

Figure 5.4   (a) Microphone configuration and (b) source plot for a spiral array.

The source plot of the spiral array, shown in figure 5.4 (b), accurately shows the location of the two sources with virtually no side lobes. This configuration has the preferred characteristic of a varying element spacing and, therefore, it can be expected to provide good results over a wide range of frequencies.

6   AIRCRAFT TEST AND RESULTS

Aircraft measurements were done to verify if the requirements are met and if the system performs adequately in practice. Aircraft flyover measurements were performed at two locations, Rotterdam-The Hague Airport and Schiphol Airport. The array was placed as close as possible to and in line with the runway. All aircraft fly over at an altitude of approximately 40 m at both airports. During the tests different array configurations were used and various types of aircraft were measured. An overview of the measurements is given in table 6.1.

Table 6.1   Overview of performed aircraft tests.

Date and Time	Array Configuration	Measured Aircraft	Airport
17-6-2011 13:31	Spiral	Antonov AN-12	Rotterdam
17-6-2011 14:46	Spiral	Dornier 328-100	Rotterdam
17-6-2011 14:54	Spiral	Boeing 737	Rotterdam
17-6-2011 15:27	Small rectangular	Boeing 737	Rotterdam
17-6-2011 16:01	Semi-circular	Boeing 737	Rotterdam
20-6-2011 17:18	Rect: spacing 3 x 5.2 cm	Airbus A321	Schiphol
20-6-2011 17:18	Rect: spacing 3 x 5.2 cm, 90°	Fokker 100	Schiphol
20-6-2011 17:53	Rect: spacing 1 x 5.2 cm	Avro/BAe 146	Schiphol

The data obtained during the tests were processed with the conventional beamformer. Because not every aircraft emits noise at the same frequencies, the frequency band which yields the best results is different for each test.
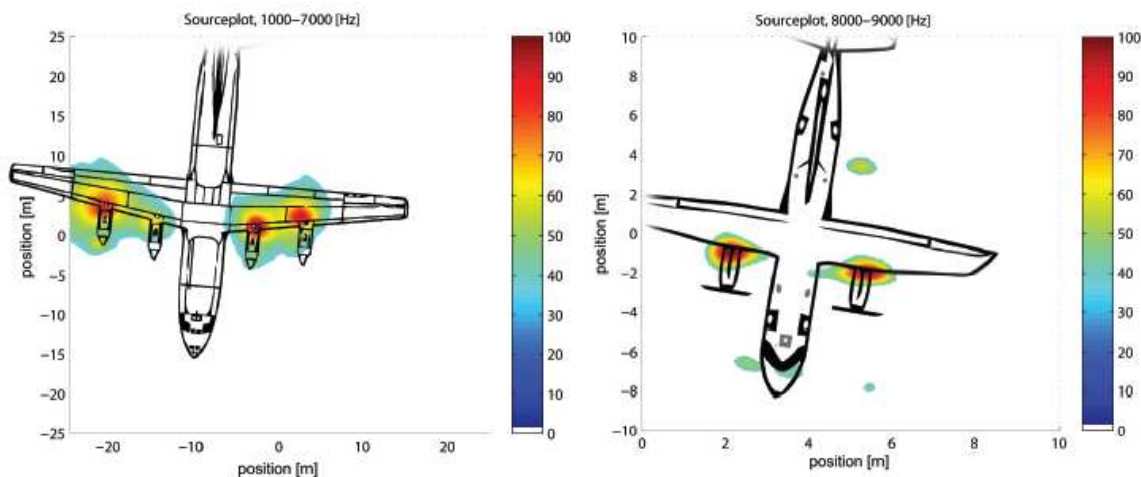
Figure 6.1   Source plot of an Antonov AN-12.   Figure 6.2   Source plot of a Dornier 328.

In the following the eight individual measurements are discussed briefly.

Figure 6.1   Antonov aircraft with four propeller engines, spiral array.
All engines are resolved, but no airframe noise was identified. This is probably because for this type of airplane the noise of the engines is much louder and more concentrated than the aerodynamic noise.

Figure 6.2   Dornier 328, spiral array.
The image is made with only high frequencies, which is probably why only the engines are found.
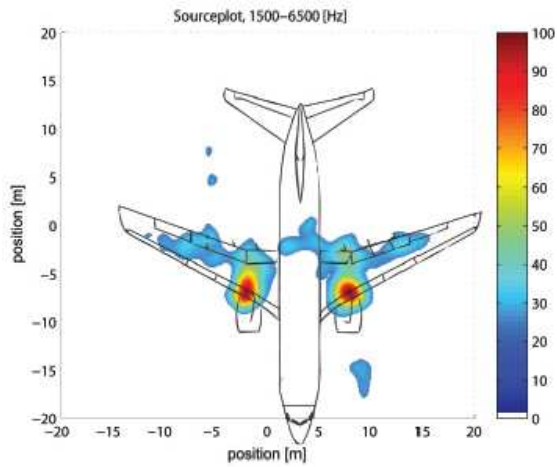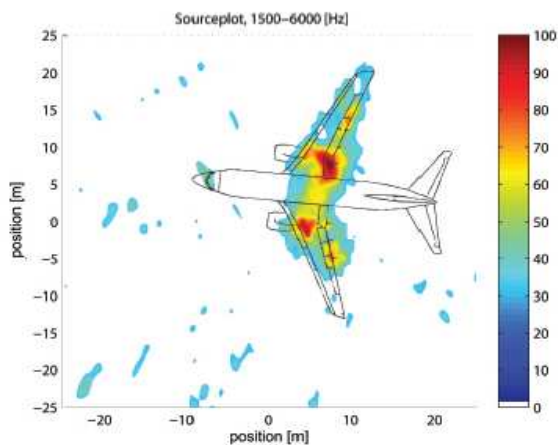
Figure 6.3   Source plot of a Boeing 737.
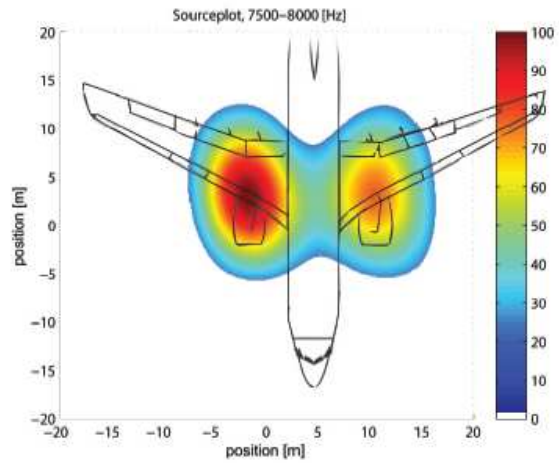
Figure 6.4   Source plot of a Boeing 737.

Figure 6.3   Boeing 737, spiral array.

The engines are clearly found as intense sources and some aerodynamic noise is found on the wing, primarily around the flaps, as expected.

Figure 6.4   Boeing 737, rectangular array with a microphone spacing of 2.6 cm.

Only the engines are found as sources. This is probably due to the high frequency range, which is much higher than the frequency range in which aerodynamic noise is emitted. However, the resolution is low in comparison to the result shown figure 5.3 obtained with the spiral array.


Figure 6.5   Source plot of a Boeing 737.
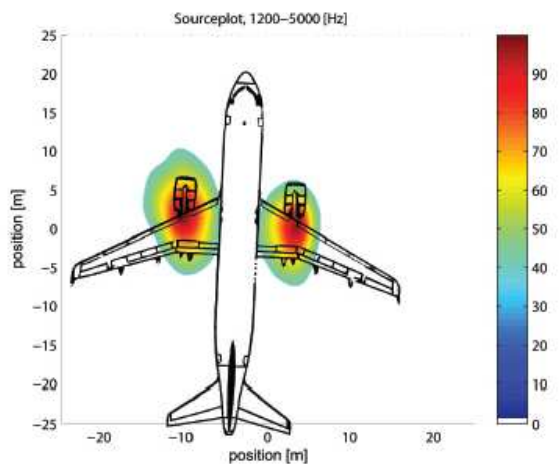
Figure 6.6   Source plot of an Airbus A321.
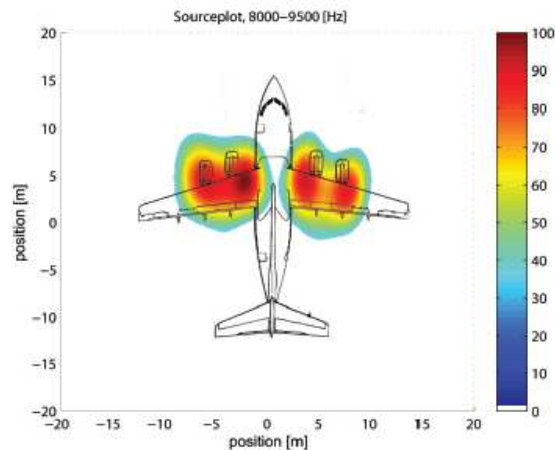
Figure 6.5   Boeing 737, semi-circular array.
One can identify the engines and the flaps. Furthermore, a source is found at the nose, which may be due to the nose wheel. However, a lot of side lobes exist, which makes the sources on the airplane questionable.

Figure 6.6   Airbus A321, rectangular array with a microphone spacing of 15.6 cm.
The engines are found with an acceptable resolution, but no aerodynamic noise is found.
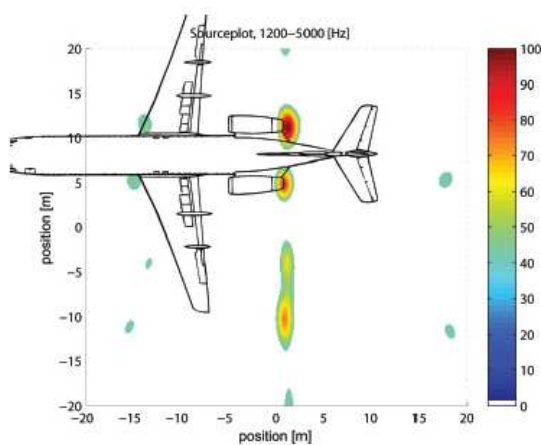
Figure 6.7   Source plot of a Fokker 100.   *Figure 6.8 Source plot of British Aerospace 146.*

Figure 6.7   Fokker 100, rectangular array with a spacing of 15.6 cm, array turned 90$^\text{o}$.
The engines are found, but no aerodynamic noise is identified. The other dots in the figure are clearly due to aliasing, which results in a symmetrical pattern of sources when a rectangular array is used. This picture shows the danger of aliasing, because the dots at the root of the wings might be interpreted as sound sources. However, from the symmetry of the picture it is clear that these dots are side lobes. The aliasing is less when the figure is made for lower frequencies, but that reduces the resolution.

Figure 6.8   British Aerospace 146, rectangular array with a spacing of 5.2 cm.
The engines are found as noise sources, but no aerodynamic noise is found. The resolution of this image is relatively low, which is probably due to the small array size.

These tests show that the spiral configuration gives the best results. Since the spiral array also performed best in the synthetic test, this configuration is preferred for future aircraft measurements.


7   CONCLUSIONS

The final design of the acoustic camera, used for the measurements shown in the previous section, is shown in figure 7.1. The corresponding camera specifications are determined and listed in table 7.1 below. It can be concluded that the requirements stated in the introduction

are met with the angular resolution even somewhat better than required. Also, from the flyover tests it can be concluded that this camera yields good results in terms of resolution and precision. Comparing our results with acoustic cameras currently on the market [9], [10], it can be stated that the specifications are fairly similar.

Table 7.1   Specifications of the acoustic camera.

Angular resolution	0.95˚ (at 6000 Hz)
Frequency range	45 Hz – 11 kHz
Array size	238 x 160 cm
Measurement time (max)	3.6 s
Dynamic range	60 dB – 126 dB
Number of microphones	32
Cost	< € 7000

We also tested which array configuration was most suitable to identify aircraft noise sources. It was found that both for the synthetic test and for a real aircraft flyover test, the spiral array gave the highest resolution and the least amount of side lobes.
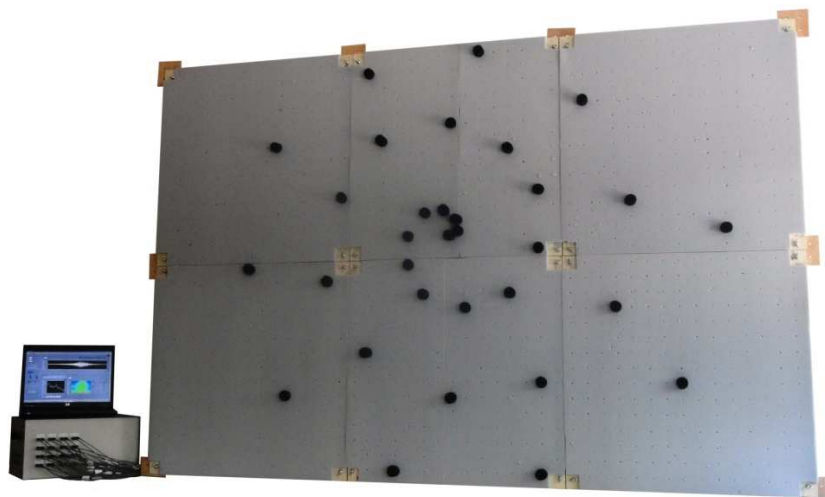
Figure 7.1   Final acoustic camera prototype system.

REFERENCES

[1]   Merford Noise Control, "Flamex Basic".
       http://www.noisecontrol.nl/media/newmedia/bestanden/Flamex%20Basic%20NL%20(
       NCS.P.1310.1.1).pdf, obtained May 2011

[2]   G. Ruijgrok, *Elements of Aviation Acoustics*, VSSD, 2007

[3]   M. Boon et al., "Final report: Seeing with sound". Technical report TU Delft faculty of
       aerospace engineering, July 2011

[4]   J. Zillman and C. Cariou, "Array Analysis For Aircraft Fly-over Measurements", Berlin
       Beamforming Conference, 2010

[5]   P. Sijtsma, "Phased array beamforming applied to wind tunnel and fly-over test", tech.
       rep. National Aerospace Laboratory, December 2010

[6]   J. Li and P. Stioca, *Robust Adaptive Beamforming*, John Wiley & Sons, 2006

[7]   D. K. Campbell, "Adaptive beamforming using a microphone array for hands-free
       telephony", February 1999

[8]   P. Sijtsma, "Clean based on spatial source coherence", *International journal of
       aeroacoustics*, vol. 6, December 2007

[9]   Norsonic, "Nor848 Acoustic Camera".
       http://www.norsonic.com/uploads/kundefiler/Downloads/pd848ed1rev1eng0610.pdf,
       obtained February 6th, 2012

[10]   gfai tech GmbH, "Acoustic Camera, Listening with your eyes".
       http://www.maschinendoktoren.at/files/akustische_kamera_brochure_english.pdf,
       obtained February 6th, 2012